JACS
JOURNAL OF THE AMERICAN CHEMICAL SOCIETY
Article
pubs.acs.org/JACS

Synthesis of Ag Nanocubes 18−32 nm in Edge Length: The Effects of Polyol on Reduction Kinetics, Size Control, and Reproducibility

Yi Wang,[†,‡] Yiqun Zheng,[§] Cheng Zhi Huang,[‡] and Younan Xia*[,†,§,¶]

[†]The Wallace H. Coulter Department of Biomedical Engineering, Georgia Institute of Technology and Emory University, Atlanta, Georgia 30332, United States

[‡]Education Ministry Key Laboratory on Luminescence and Real-Time Analysis, College of Chemistry and Chemical Engineering, Southwest University, Chongqing 400715, P. R. China

[§]School of Chemistry and Biochemistry, Georgia Institute of Technology, Atlanta, Georgia 30332, United States

[¶]School of Chemical and Biomolecular Engineering, Georgia Institute of Technology, Atlanta, Georgia 30332, United States

Supporting Information

ABSTRACT: This article describes a robust method for the facile synthesis of small Ag nanocubes with edge lengths controlled in the range of 18−32 nm. The success of this new method relies on the substitution of ethylene glycol (EG)—the solvent most commonly used in a polyol synthesis—with diethylene glycol (DEG). Owing to the increase in hydrocarbon chain length, DEG possesses a higher viscosity and a lower reducing power relative to EG. As a result, we were able to achieve a nucleation burst in the early stage to generate a large number of seeds and a relatively slow growth rate thereafter; both factors were critical to the formation of Ag nanocubes with small sizes and in high purity (>95%). The edge length of the Ag nanocubes could be easily tailored in the range of 18−32 nm by quenching the reaction at different time points. For the first time, we were able to produce uniform sub-20 nm Ag nanocubes in a hydrophilic medium and on a scale of ∼20 mg per batch. It is also worth pointing out that the present protocol was remarkably robust, showing good reproducibility between different batches and even for DEGs obtained from different vendors. Our results suggest that the high sensitivity of synthesis outcomes to the trace amounts of impurities in a polyol, a major issue for reproducibility and scale up synthesis, did not exist in the present system.

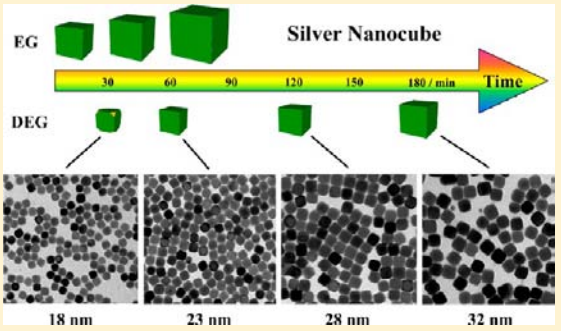

1. INTRODUCTION

Noble-metal nanocrystals have received ever increasing attention in recent years due to their remarkable physicochemical properties that are often substantially different from those of bulk materials.[1−5] Silver nanocrystals, in particular, have been a subject of intensive research owing to their great performance in a broad range of applications involving localized surface plasmon resonance (LSPR), surface-enhanced Raman scattering (SERS), metal-enhanced fluorescence, sensing, imaging, catalysis, and antimicrobial technology.[6−13] It has been established that the physicochemical properties of Ag nanocrystals are strongly dependent on their size, shape, and morphology. As such, many studies have been dedicated to the syntheses of Ag nanocrystals with well-controlled sizes and shapes. Thanks to the efforts from many research groups, Ag nanocrystals can now be prepared with a myriad of different shapes or morphologies, with notable examples including spheres, cubes, bars, octahedrons, right bipyramids, decahedrons, rods/wires with a pentagonal cross section, and concave cubes or octahedrons, among others.[14−16] Among them, Ag nanocubes have received particular interest owning to their sharp corners beneficial to both LSPR and SERS applications; their use as seeds with well-defined facets for directing overgrowth; and their unique use as sacrificial templates for galvanic replacement to generate hollow nanostructures (e.g., Ag−Au nanoboxes and nanocages) for a variety of applications.[17−25]

Over the past decade or so, a number of different methods have been demonstrated for the synthesis of Ag nanocubes. For example, our group pioneered the synthesis of Ag nanocubes via polyol reduction in ethylene glycol (EG) in 2002.[26] This one-pot strategy was further improved thereafter by introducing a trace amount of sulfide (S^{2-}) or hydrosulfide (HS^-) into the chloride-mediated polyol synthesis and by switching the precursor compound from silver nitrate ($AgNO_3$) to silver trifluoroacetate (CF_3COOAg).[27−33] With these modifications, we were able to generate Ag nanocubes with tunable edge lengths in the range of 30−70 nm. Recently, the upper limit of size was further extended to 200 nm and beyond by switching to a seed-mediated approach.[34] In addition to the polyol reduction, other strategies such as hydrothermal synthesis and

Received: November 23, 2012
Published: January 14, 2013

   dx.doi.org/10.1021/ja311503q | J. Am. Chem. Soc. 2013, 135, 1941−1951

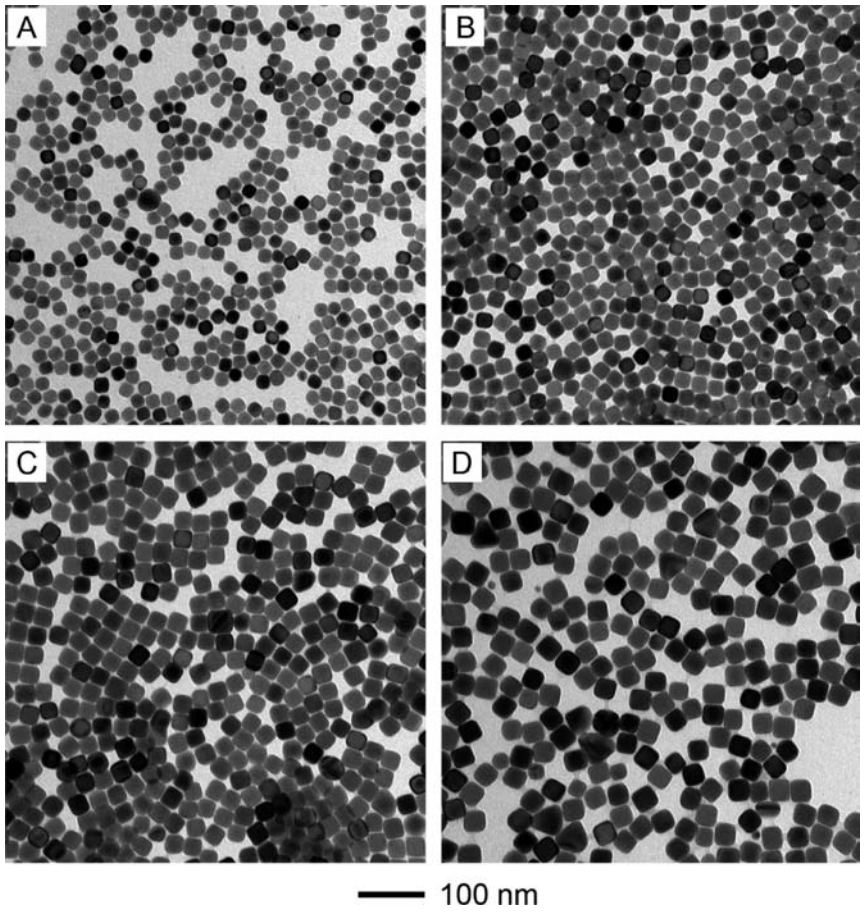

Figure 1. TEM images of Ag nanocubes obtained at different reaction times of a standard synthesis in DEG: (A) 30, (B) 60, (C) 120, and (D) 180 min. The nanocubes had edge lengths of (A) 18, (B) 23, (C) 28, and (D) 32 nm, respectively.

solid−liquid interface synthesis have also been reported for the preparation of Ag nanocubes.[35−37] Despite these successful demonstrations, it remains a grand challenge to synthesize uniform Ag nanocubes with edge length below 30 nm. This technical challenge can be attributed to three possible sources: (*i*) It is very hard to terminate the growth process due to the intrinsic autocatalytic activity of Ag nanocrystals, unless the precursor has been completely consumed. In that case, the Ag nanocrystals can quickly grow into relatively large sizes. (*ii*) Small Ag nanocubes tend to lose their sharp corners due to the high sensitivity of Ag toward oxidative etching caused by the oxygen from air. (*iii*) The high mobility of Ag atoms often facilitates the transformation of small Ag nanocubes into a thermodynamically more stable shape such as cuboctahedron when there is no sufficient capping for the {100} facets. To date, there is only one publication on the reproducible synthesis of Ag nanocubes (truncated at corners) with edge lengths below 30 nm, which was conducted in isoamyl ether by introducing Fe(III) species as an oxidative etchant to eliminate twinned seeds.[38] However, the Ag nanocubes obtained using this protocol were dispersed in a hydrophobic solvent and they could not be directly used with a hydrophilic system without going through a ligand exchange process, which is often troubled by problems such as low efficiency of phase transfer, possible irreversible aggregation of nanoparticles, as well as permanent alterations to the shape and related properties.[39−41] In addition, the previously reported polyol methods are often troubled by the unexpected impurities contained in the commercial reagents. Taking EG as an example, due to its synthesis and storage in steel vessels, it is often contaminated by trace amounts of Fe(II) or Fe(III) species.[4] Both of them can induce or influence oxidative etching by coupling with the O_2 from air, causing problems for reproducibility and scale-up production. Taken together, it is not hard to understand why it has been so difficult to develop a robust and reliable method for generating uniform Ag nanocubes smaller than 30 nm in edge length, in a hydrophilic phase, and with high purity.

In the present work, we accomplished the synthesis of Ag nanocubes with uniform and controllable edge lengths below 30 nm by using diethylene glycol (DEG) rather than EG as both a solvent and a reductant. The edge lengths of the Ag nanocubes could be easily tuned in the range of 18−32 nm by quenching the reaction at a specific time point with the assistance of a UV−vis spectrometer. Different from the previous methods based on EG, the use of DEG offers a nucleation burst to generate a high concentration of Ag nuclei/seeds in the early stage and then a much slower growth rate thereafter. The use of polyols with longer hydrocarbon chains—for example, triethylene glycol (TEG) and tetraethylene glycol (TTEG)—only led to the formation of twinned particles with irregular shapes, implying that the production of small Ag nanocubes with uniform sizes is highly sensitive to the reaction kinetics. To our knowledge, this is the first time that Ag nanocubes could be synthesized in a hydrophilic phase with the edge lengths being pushed down to the sub-20 nm regime. Moreover, this new method based on DEG is highly robust and

reproducible, and could be easily scaled up while maintaining high purity (typically, >95%) for the final products. Owing to their small sizes and high purity, the as-prepared Ag nanocubes were further employed as templates to prepare Ag−Au bimetallic nanostructures with hollow interiors via a galvanic replacement reaction. Such small and hollow nanostructures with tunable LSPR properties are expected to show enhanced performance in a number of *in vivo* applications that include drug delivery, optical imaging, and photothermal therapy.

2. EXPERIMENTAL SECTION

Chemicals and Materials. Diethylene glycol (DEG, ≥99.0%) involved in the standard synthesis was obtained from Sigma-Aldrich (lot no. BCBF4248 V) while DEG used for the comparison study was obtained from J. T. Baker (lot no. K02621). Triethylene glycol (TEG, ≥99.0%), tetraethylene glycol (TTEG, 99%), silver trifluoroacetate (CF_3COOAg, ≥99.99%), sodium hydrosulfide hydrate ($NaHS{\cdot}xH_2O$), aqueous hydrochloric acid solution (HCl, 37%), hydrogen tetrachloroaurate(III) hydrate ($HAuCl_4{\cdot}3H_2O$), poly(vinyl pyrrolidone) (PVP, $M_W \approx 55\,000$), poly(ethylene glycol) methyl ether (mPEG, $M_n \approx 1000$), formaldehyde (37 wt % in H_2O), and sodium chloride were all obtained from Sigma-Aldrich. Deionized (DI) water with a resistivity of 18.2 MΩ·cm was used throughout the experiment. The standard synthesis of Ag nanocrystals was carried out in a 100 mL flask with round-bottom (ACE Glass).

Synthesis of Ag Nanocubes in DEG. In a standard synthesis, 5 mL of DEG was added into a flask and heated under magnetic stirring in an oil bath set to 150 °C for 30 min. Other reagents were separately dissolved in DEG and sequentially introduced into the flask using a pipet. Specifically, 0.06 mL of NaSH solution (3 mM) was added first. After 4 min, 0.5 mL of HCl (3 mM) was added, followed by 1.25 mL of PVP (20 mg/mL). After another 2 min, 0.4 mL of CF_3COOAg solution (282 mM) was introduced. During the entire process, the flask was capped with glass stoppers except for the addition of reagents. The synthesis was quenched by placing the flask in an ice−water bath and the products were collected by centrifugation, followed by washing with acetone and then DI water to remove the remaining precursor, DEG, and excess PVP. We controlled the sizes of the Ag nanocubes by monitoring the position of their major LSPR peak using a UV−vis spectrometer. Briefly, a small amount (a few drops) of the reaction solution was taken out from the flask using a glass pipet and diluted with 1 mL DI water in a cuvette. The extinction spectrum was recorded and compared with the calibration curve to determine the size of the nanocubes.

Synthesis of Au Nanoframes and Nanocages Using the Ag Nanocubes as Templates. The Au nanoframes and nanocages were prepared via a galvanic replacement reaction between the as-prepared Ag nanocubes and an aqueous $HAuCl_4$ solution. In a typical process, 100 μL of the Ag nanocubes (1.5×10^{13} particles/mL) was dispersed in 5 mL of DI water containing 1 mg/mL PVP and heated to 90 °C. A specific amount of 0.1 mM $HAuCl_4$ aqueous solution was then added using a syringe pump at a rate of 10 mL/h under magnetic stirring. We recorded the UV−vis spectra to track the progress of the reaction as the volume of $HAuCl_4$ solution was increased. The as-prepared sample was washed with 10 mL saturated solution of NaCl to remove AgCl. Finally, the product was centrifuged and washed with DI water three times and then dispersed in DI water for further characterization.

Instrumentation. Transmission electron microscopy (TEM) images were taken using a Hitachi H-7500 microscope operated at 75 kV. Extinction spectra of all the Ag nanocrystals were recorded using a Varian UV−vis spectrometer (Cary 50). The concentration of Ag was determined using a Perkin-Elmer inductively coupled plasma mass spectrometer (ICP-MS, NexION 300Q) and then converted to the concentration of Ag nanocubes once the particle size had been determined from TEM imaging. An Eppendorf centrifuge (5430) was used for the centrifugation and washing of all samples.

3. RESULTS AND DISCUSSION

Synthesis and Size Control of Small Ag Nanocubes in DEG. Figure 1 shows TEM images of the Ag nanocubes that were obtained at different stages of a standard synthesis in DEG. The edge lengths increased from 18 to 32 nm. After the addition of CF_3COOAg for 30 min, we obtained Ag nanocubes with an edge length of 18 nm (15% truncation at corners, which was calculated by cutting the cube with a sphere whose radius was 85% of the distance from the particle's center to its apex).[42] When the reaction time was prolonged to 60, 120, and 180 min, the edge lengths of the Ag nanocubes increased to 23, 28, and 32 nm, respectively. In this new synthesis, the relatively slow growth rate made it feasible to finely tune the size of the Ag nanocubes and therefore obtain uniform nanocubes with a specific size sought for a particular application. Compared to previously reported methods, the relatively slow growth rate of Ag nanocubes in the present work represents a major advantage. For example, the NaSH-mediated polyol method for the synthesis of Ag nanocubes in EG was typically completed in 8−10 min, and it only took roughly 2 min for the nanocubes to grow from 25 to 45 nm.[29,32] The fast growth rate makes it very hard to monitor the size of Ag nanocubes during a synthesis, and it was impractical to stop the reaction at an appropriate time to obtain nanocubes with a specific size. On the other extreme, the HCl-mediated polyol synthesis of Ag nanocubes in EG usually took 16−25 h to generate well-developed nanocubes,[27] which is not only time-consuming but also impractical for size control. A few years ago, we developed a new approach based on EG to Ag nanocubes of 30−70 nm in edge length with CF_3COOAg as a precursor, and this synthesis typically took a duration of 15−90 min to complete.[33] Although a relatively slow growth rate was achieved in this method, the reaction was still too fast in the early (typically within the first 15 min) stage of a synthesis to control. As a result, it could not be used to obtain Ag nanocubes with edge lengths less than 30 nm. In the present synthesis, the slower reduction kinetics in DEG allowed us to prolong the formation of Ag nanocubes over a longer period of time (180 min vs 30 min). As a result, we could easily monitor the growth of Ag nanocubes and finely tune their sizes in the range below 30 nm by simply varying the growth time with the aid of a UV−vis spectrometer. More importantly, as shown by the TEM images in Figure 1, all the as-obtained Ag nanocubes were very uniform in size, and the purity of cubic shape exceeded 95% for all the samples. The achievement of such a small and uniform size for the Ag nanocubes could be attributed to the rapid formation of a high concentration of Ag nuclei or seeds in DEG, followed by growth of the seeds at a relatively slow rate.

The uniform Ag nanocubes with controlled edge lengths allowed us to systematically investigate their LSPR properties as a function of size. Figure 2A shows the normalized UV−vis extinction spectra recorded from aqueous suspensions of the Ag nanocubes shown in Figure 1. The major LSPR peaks displayed a constant red-shift from 401 to 407, 413, and 418 nm as the size of the nanocubes increased. A shoulder peak at ∼355 nm appeared after 30 min, suggesting that Ag nanocubes with sharp corners started to form at this point, which was in agreement with our previous observation during the synthesis of Ag nanocubes in EG.[33] This shoulder peak became more obvious to observe with the increase of reaction time, indicating that the corners of the Ag nanocubes were increasingly sharpened during the further growth. Significantly, there was a linear

dx.doi.org/10.1021/ja311503q | J. Am. Chem. Soc. 2013, 135, 1941−1951

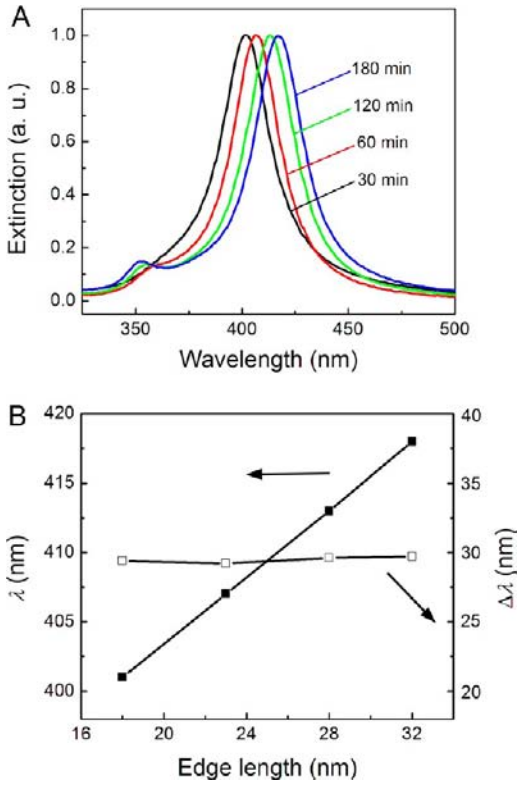

Figure 2. (A) UV−vis spectra of Ag nanocubes shown in Figure 1, which had different edge lengths. (B) Plots showing the wavelength (λ) of the major LSPR peak (solid symbols) and the full width at half-maximum ($\Delta\lambda$) of the major LSPR peak (hollow symbols) as a function of the edge length (L) of Ag nanocubes. The fitting curve for solid symbols can be expressed as $\lambda = 1.212L + 379.1$ ($R^2 = 0.9999$), which was used to calculate the edge length of Ag nanocubes from the major LSPR peak position derived from the UV−vis spectrum.

relationship between the major LSPR peak position and the edge length of the Ag nanocubes (Figure 2B). The fitting curve could be expressed as $\lambda_{max} = 1.212L + 379.1$ ($R^2 = 0.9999$), where λ_{max} and L are the major LSPR peak position and the edge length, respectively. In practice, we can obtain Ag nanocubes with a specific size by constantly checking the UV−vis spectra taken at different reaction stages. Since the growth rate of Ag nanocubes in DEG was reasonably slow, their edge lengths could be controlled with an accuracy of 1−2 nm by using the UV−vis spectroscopic method. In addition, the other plot in Figure 2B shows that the full width at half-maximum ($\Delta\lambda$) for the major LSPR peak of the Ag nanocubes was as narrow as ∼30 nm and essentially did not change as the nanocubes grew in size, suggesting that the nanocubes were maintained with the same size and shape uniformity during their growth. Taken together, it can be concluded that uniform Ag nanocubes with specific sizes could be readily obtained by stopping the reaction at different time points.

We also optimized the synthesis by adjusting the reaction temperature and the amount of PVP added into the reaction system. When the synthesis was performed at 130 and 170 °C while other parameters were kept the same as the standard procedure, the products showed a mixture of Ag nanocubes and nanoparticles of other shapes (see Figure S1, A and B, in the Supporting Information). On the other hand, it was found that the amount of PVP in the synthesis also affected the purity of nanocubes. When the mole ratios of PVP to CF_3COOAg was 4:1 or 1:1, a small amount of other types of nanoparticles such as rods, spheres, and irregular particles were obtained (Figure S1, C and D). These results suggest that 150 °C and a mole ratio of 2:1 between PVP and CF_3COOAg in the standard procedure seemed to be the optimal conditions. In addition, like the synthesis of Ag nanocubes in EG, it was found that NaSH and HCl both played important roles in the new protocol. As shown in Figure S2, twinned nanoparticles with irregular shapes were obtained in the absence of both NaSH and HCl, or either one of them (a small number of nanorods and nanocubes also formed in the synthesis without adding NaSH). The corresponding LSPR peaks were much broader than what was observed for the Ag nanocubes prepared using the standard procedure, suggesting that the size/shape variations of these Ag nanoparticles were broader. Moreover, no obvious peak around 355 nm was observed in the extinction spectra, indicating that the Ag nanoparticles in these samples did not have sharp corners. Combined together, it can be concluded that both NaSH and HCl were critical to the successful synthesis of small Ag nanocubes with sharp corners and in high yield/purity.

Although several methods have been reported for the synthesis of Ag nanocubes, most of them were plagued by limitations such as low throughput, low yield/purity, as well as poor robustness and reproducibility. By manipulating the reduction kinetics with DEG, we could not only finely tune the edge length of the Ag nanocubes to a region below 30 nm but also achieve high yield and purity (typically, >95%) for the sample, together with good robustness, high reproducibility, and scale-up capability. Figure 3A shows the extinction spectra of Ag nanocubes prepared in five separate batches using the standard procedure where the reactions were all stopped at t = 60 min after the addition of Ag precursor. It is clear that their spectra (curves 1 to 5) overlapped reasonably well, indicating that the present method did have good reproducibility for the synthesis of small Ag nanocubes in terms of size/shape uniformity and corner sharpness. We also conducted a 10× scale-up synthesis to evaluate the capability of this new method for high-volume production of Ag nanocubes. The extinction spectrum of the Ag nanocubes is shown in Figure 3A as curve 6, which also overlapped well with the spectra of other samples obtained using the standard procedure. The TEM image in Figure 3B clearly shows that uniform Ag nanocubes with high purity (>95%) was also obtained in the scale-up synthesis. The setup used for the scale-up synthesis and the final suspension of Ag nanocubes are shown in Figure S3. The capability of this method for scale-up synthesis will play an important role in developing various applications of such small Ag nanocubes. Other than the DEG supplied by Sigma-Aldrich in the standard synthesis, we have also tested DEG obtained from J. T. Baker to demonstrate the robustness of this new protocol. On the basis of the result shown in Figure S4, we can claim that small Ag nanocubes with high purity and size/shape uniformity could still be obtained, suggesting that the unexpected trace impurities in polyol was not an issue at all in the polyol synthesis based on DEG.

To better understand the nucleation and growth of Ag nanocubes in DEG, aliquots were taken at different time points of the early (<30 min) stage in a standard synthesis and the samples were then analyzed using TEM. After the addition of Ag precursor, the colorless solution became whitish, immediately followed by a light yellow color, suggesting that a burst of nucleation occurred, during which a large number of nuclei

dx.doi.org/10.1021/ja311503q | J. Am. Chem. Soc. 2013, 135, 1941−1951

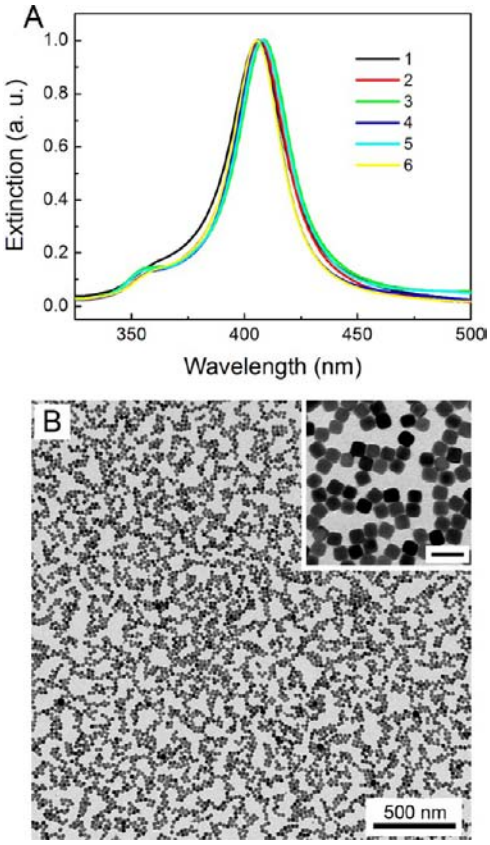

Figure 3. Demonstration of reproducibility and scale-up capability for the synthesis of small Ag nanocubes in DEG: (A) UV−vis spectra of five different batches of nanocubes prepared using the standard procedure (curves 1−5) and of the nanocubes produced in a 10× scale-up synthesis (curve 6); and (B) low-magnification and high-magnification (inset) TEM images of the Ag nanocubes obtained in the scale-up synthesis. The scale bar in the inset is 50 nm.

were formed in a short period of time. As shown by TEM images in Figure 4, some large particles (~80 nm) still existed at t = 3 min, together with a few small particles. This observation was consistent with our previous synthesis of Ag nanocubes in EG, where it was established that both the formation of AgCl particles (the large ones) and the birth of single-crystal Ag seeds (the small ones) occurred simultaneously in the early stage of a synthesis.[33] The number and size of the large AgCl particles decreased with the reaction time, accompanied by the increase of small Ag seeds in terms of both size and number. At t = 10 min, all the AgCl particles had disappeared and only small Ag nanospheres with a diameter of 12 nm were observed in the system. Afterward, the nanospheres increased in size at a relatively slow rate and nanocubes with an edge length of 18 nm started to appear at t = 30 min.

Comparison of Different Polyols for the Synthesis. It is clear that single-crystal Ag seeds could be obtained in high purity during the nucleation stage for both the EG and DEG systems.[33] However, a slower growth rate could be achieved in DEG than in EG. The slower kinetics associated with the growth of Ag nanocubes in DEG could be attributed to a longer hydrocarbon chain and thus weaker reducing power in comparison with EG.[43,44] It is thus interesting to see whether uniform Ag nanocrystals with smaller sizes can also be obtained in other polyols with longer hydrocarbon chains than DEG. To address this important issue, we compared the synthesis of Ag nanocrystals in polyols with different lengths of hydrocarbon chains. The chemical structures of these polyols were summarized in Figure S5. Like in the standard procedure used for DEG, we also investigated the time-dependent evolution of Ag nanocrystals in TEG and TTEG. As shown by the TEM images in Figure 5, both large AgCl particles (~100 nm) and a few small Ag nanocrystals were formed in TEG at t = 1 min, which is similar to what was observed during the synthesis in DEG. At t = 10 min, the AgCl particles disappeared and small Ag nanocrystals with two major sizes were observed. One was around 22 nm and the other was below 5 nm. It should be noted that most of the larger particles (~22 nm) contained twin defects, and they tended to grow at a relatively faster rate than the smaller ones. Eventually, the final product obtained at t = 2 h became a mixture of rods, bipyramids, cubes, and cuboctahedrons with two major sizes of ~41 and ~5 nm. In the case of TTEG, a mixture of AgCl and Ag nanoparticles was also observed in the early stage (Figure 6). However, after the AgCl particles had disappeared at t = 30 min, essentially all of the Ag nanoparticles (~21 nm in size) showed a twinned structure and they tended to aggregate. These twinned particles then grew into large structures with irregular shapes in a short period of time.

We also recorded UV−vis spectra of the Ag nanoparticles prepared in TEG and TTEG (Figure S6). As the reaction time increased, the LSPR peaks of Ag nanoparticles obtained in both TEG and TTEG were constantly red-shifted, suggesting that their average sizes were gradually increased. It should be noted that the full width at half-maximum of these LSPR peaks were much broader than those of Ag nanocubes prepared in DEG, indicating that the size/shape distributions of the nanoparticles prepared in TEG and TTEG were broader than the nanocubes obtained in DEG.

From the viewpoint of nucleation and growth, the concentration of Ag atoms should steadily increase with reaction time after the injection of a salt precursor, which is reduced and depleted in the presence of a reductant. Once the concentration of Ag atoms has reached the point of supersaturation, the atoms will start to aggregate into small clusters (i.e., nuclei) through homogeneous nucleation. Then, the resultant Ag nuclei will grow in an accelerated manner due to the involvement of autocatalysis, and thus, the concentration of Ag atoms in the solution will quickly drop to a level below supersaturation. As long as the concentration of Ag atoms is held below the threshold for homogeneous nucleation, no additional nucleation events will occur. Therefore, one has to fulfill the following requirements in order to obtain Ag nanocubes with a single-crystal structure and small sizes: (*i*) rapid formation of a large number of nuclei/seeds in the early stage to deplete essentially all the Ag atoms; and (*ii*) slow growth of the nuclei/seeds in the following step to allow for quenching of the synthesis once a specific size has been reached for the nanocubes. If nucleation is allowed to proceed over an extended period, the precursor will be unevenly depleted, resulting in different growth rates for the nuclei formed at different stages of a synthesis. These arguments suggest that an effective approach to the synthesis of Ag nanocrystals with uniform sizes and shapes and in high purity is to separate the nucleation and growth steps.

To achieve a brief spurt of nucleation in a polyol synthesis, one has to optimize several parameters such as the concentration of precursor, the temperature, and the reducing power of polyol. In the present work with different polyols, the

dx.doi.org/10.1021/ja311503q | J. Am. Chem. Soc. 2013, 135, 1941−1951

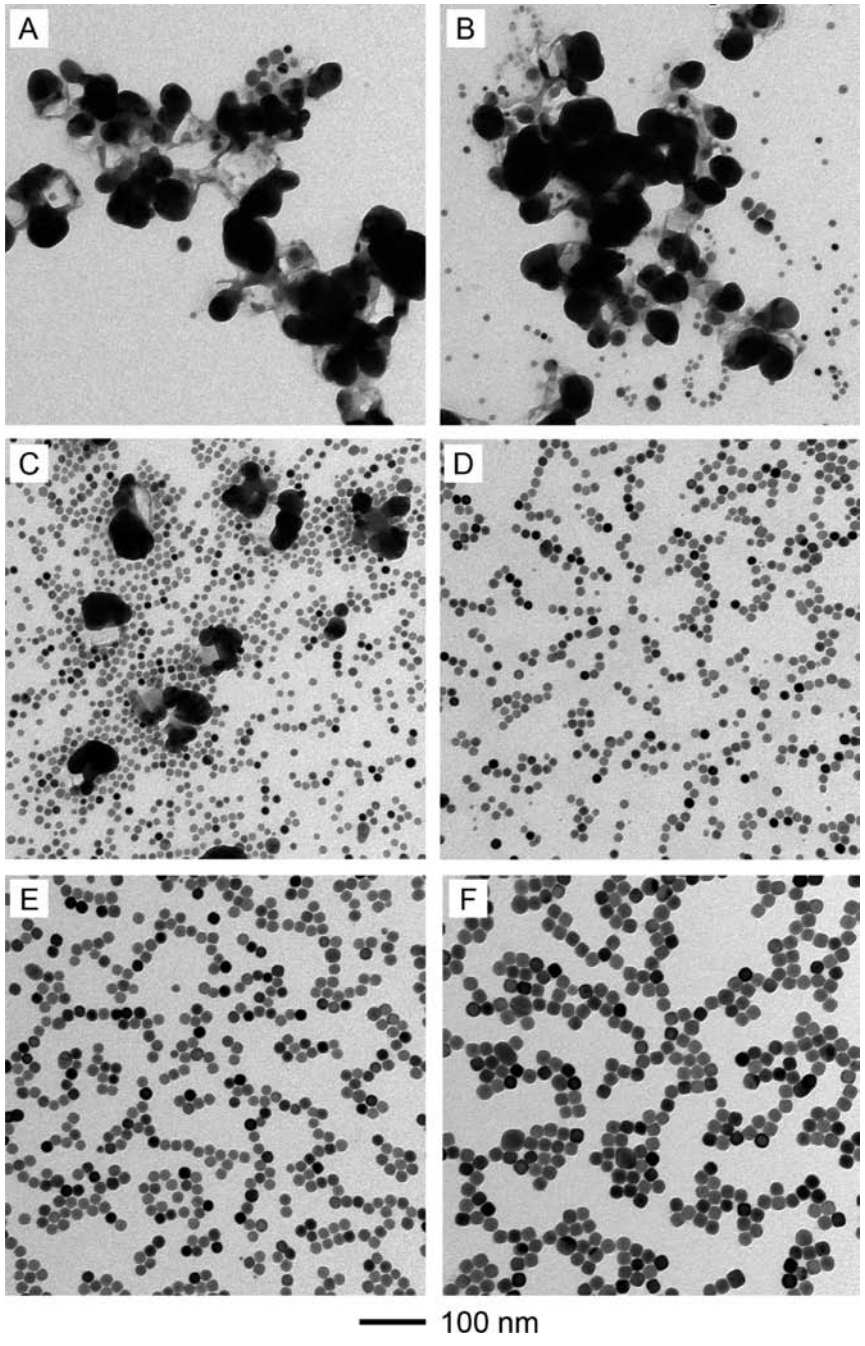

Figure 4. TEM images showing the early stages of a standard synthesis of Ag nanocubes at: (A) 1, (B) 3, (C) 5, (D) 10, (E) 20, and (F) 30 min.

concentration of precursor and temperature were both fixed. Thus, the reducing power of a polyol is expected to play the most important role in the nucleation and growth. It has been demonstrated that the longer the hydrocarbon chain of a polyol has, the weaker its reducing power will be, so the reducing powers of polyols should decrease in the order of: EG > DEG > TEG > TTEG.[43,44] Therefore, it is not hard to understand why uniform Ag seeds could be obtained in high yields in both EG and DEG. It was because a rapid nucleation burst was ensured by their relatively strong reducing powers. On the contrary, Ag nanoparticles with broad size distributions were obtained in TEG and TTEG due to their relatively weak reducing powers and thus nucleation over an extended period of time. Furthermore, the slow nucleation in TEG and TTEG led to the formation of seeds with twin defects in an effort to reduce the total surface free energy. Such a dependence of crystallinity on reaction kinetics was also observed by Lee and co-workers in the synthesis of Au nanoparticles.[45]

Although single-crystal Ag nanocubes could be obtained in both EG and DEG under appropriate conditions, one could only produce small Ag nanocubes with edge lengths below 30 nm in DEG. Except for the difference in reduction kinetics between EG and DEG, their difference in viscosity could be a major parameter responsible for the small size and good uniformity of the Ag nanocubes obtained in DEG. According to the Stokes–Einstein equation, the diffusion coefficient D of a spherical particle with radius r is related to the viscosity of the medium η by the following equation:

$$D = k_B T / 6\pi\eta r \quad (1)$$

dx.doi.org/10.1021/ja311503q | J. Am. Chem. Soc. 2013, 135, 1941–1951

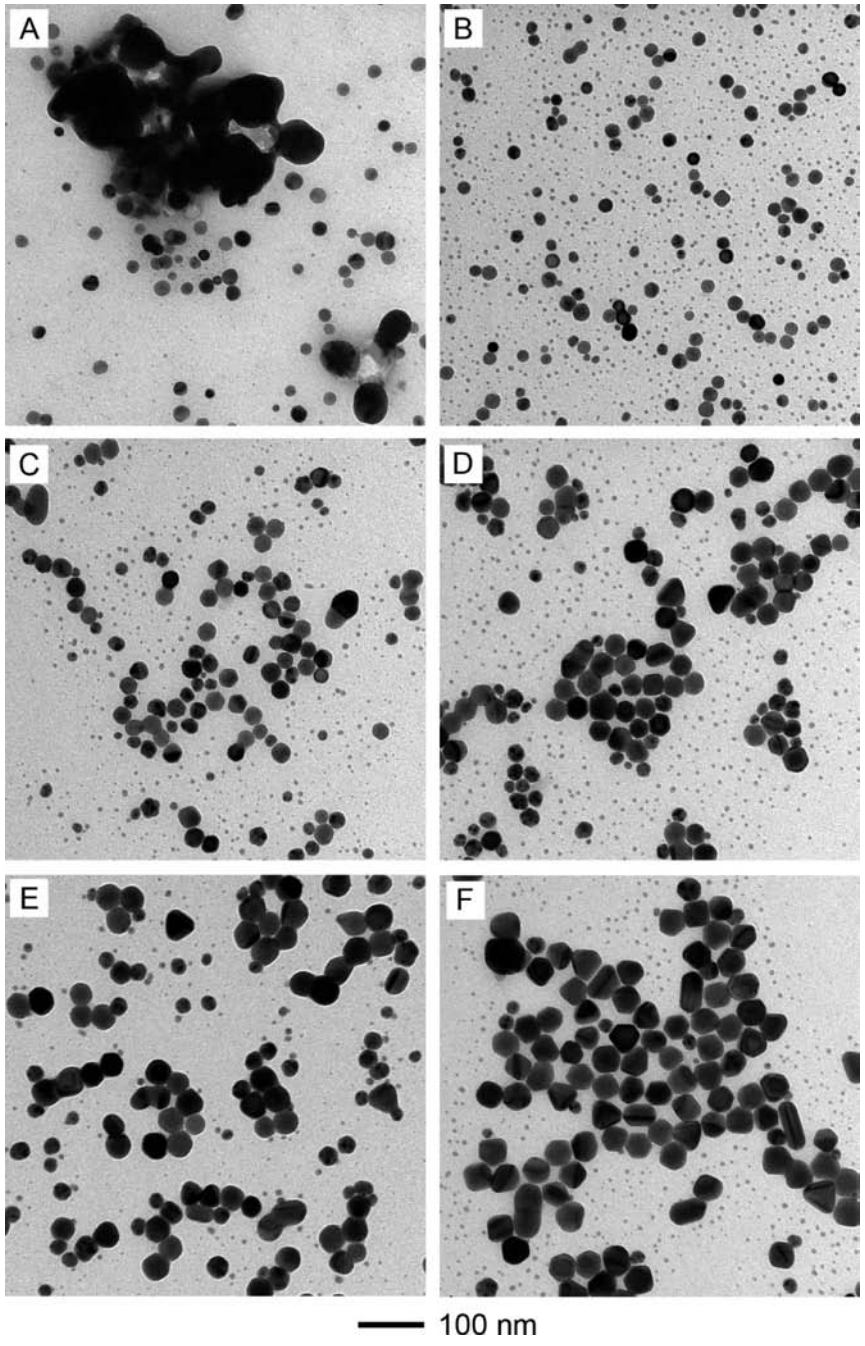

Figure 5. TEM images of Ag nanocrystals obtained from a synthesis in TEG at different time points: (A) 1, (B) 10, (C) 30, (D) 60, (E) 90, and (F) 120 min. Except for the solvent, all other parameters were kept the same as the standard procedure involving DEG.

where k_B is the Boltzmann constant and T is the absolute temperature. As expected, the diffusion rate of a Ag atom or particle in DEG is much lower as compared with that in EG owing to the difference in viscosity (1.3 vs 0.9 mPa•s for DEG and EG at 150 °C).[46,47] As a result, the probability for the Ag atoms and particles to collide is much lower in DEG than in EG, resulting in the formation of Ag nuclei/seeds at a higher concentration in the former solvent. According to the measurements by ICP-MS and TEM, the concentrations of Ag nanocubes prepared in DEG and EG were 1.5×10^{13} and 1.1×10^{12} particles/mL, respectively. Since a larger number of nuclei/seeds will consume more precursors during their growth, smaller Ag nanocubes will be obtained in DEG when the amount of Ag precursor is fixed. To understand the role of viscosity in suppressing aggregation of Ag nuclei in the initial stage of a synthesis, we also introduced a small amount of mPEG into the EG-based synthesis[33] to increase the viscosity of the system. As shown in Figure S7, the average edge length of the Ag nanocubes prepared under this condition was indeed smaller than the products obtained in the absence of mPEG (35 nm vs 45 nm), confirming the important role of solution viscosity in increasing the density of nuclei and thus reducing the size of Ag nanocubes. In addition to the benefit of higher viscosity, the slower reduction kinetics of DEG relative to EG during the growth stage allowed the seeds to grow at a relatively slow rate. Combined together, we were able to reproducibly generate small Ag nanocubes with controlled edge lengths. On the other hand, although the viscosities of TEG and TTEG are

dx.doi.org/10.1021/ja311503q | J. Am. Chem. Soc. 2013, 135, 1941−1951

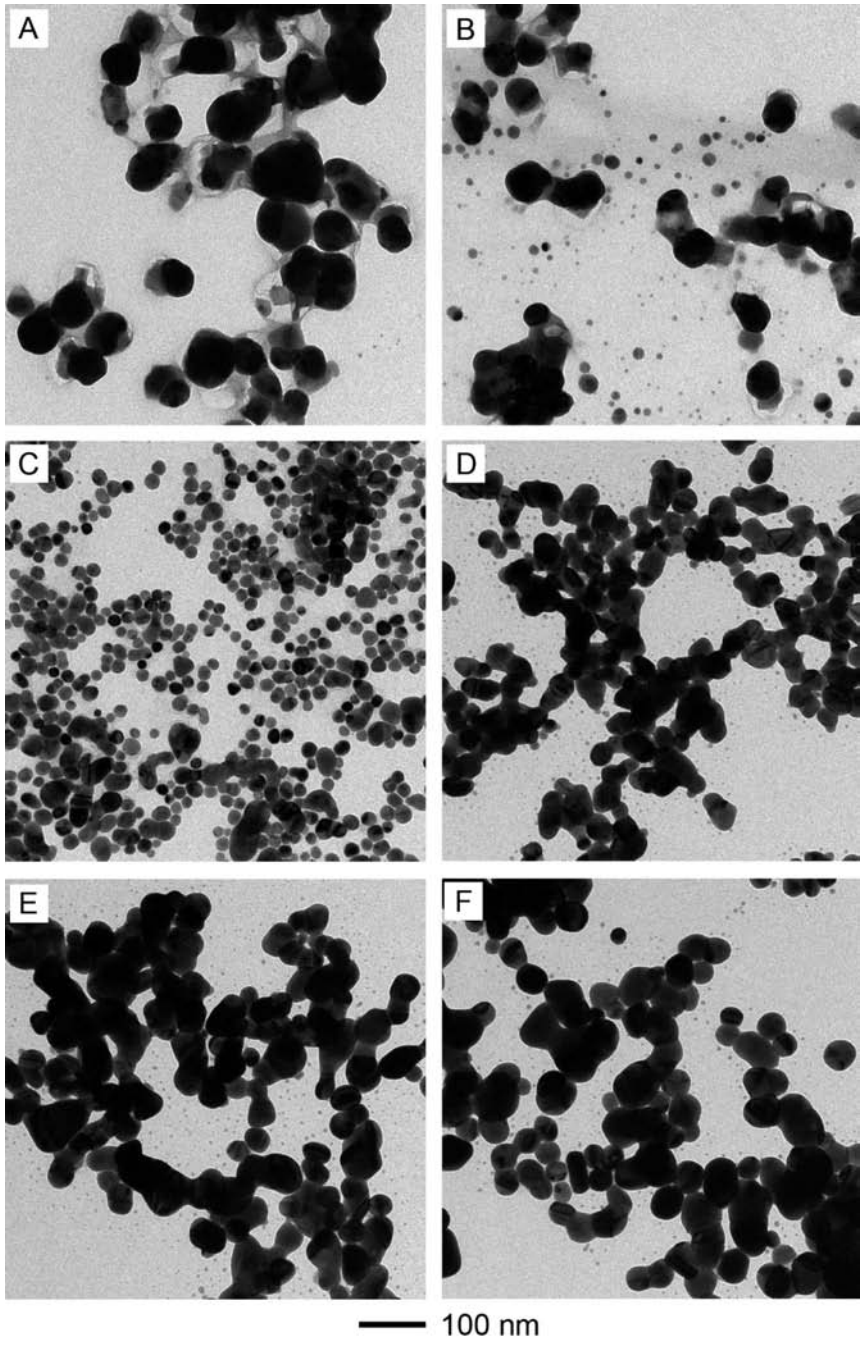

Figure 6. TEM images of Ag nanocrystals obtained from a synthesis in TTEG at different time points: (A) 1, (B) 10, (C) 30, (D) 60, (E) 90, and (F) 120 min. Except for the solvent, all other parameters were kept the same as the standard procedure based on DEG.

higher than that of DEG, the mixture of single-crystal and twinned seeds, which are formed due to the slow nucleation over a longer period of time, will grow at different rates. As a result, Ag nanoparticles with a broad size distribution and a number of different shapes were obtained when TEG or TTEG is used as the solvent.

In addition to the replacement of solvent for generating Ag nanocubes with small sizes in a polyol synthesis, it is also possible to achieve the same goal by adjusting other parameters that can influence the reduction kinetics and viscosity of an EG-based system. For example, we have tried a synthesis in EG with the addition of formaldehyde as an extraneous reductant at relatively low temperatures (100 and 130 °C), which was supposed to offer a proper reducing power and relatively high viscosity. However, we only obtained Ag nanoparticles with irregular shapes and broad size distributions under these conditions (Figure S8). This result suggested that it might be more complicated and much harder to put the synthesis under control relative to the present approach that only involved a simple change of solvent. In addition, we also tried to further manipulate the synthesis by employing mixtures of EG and DEG at different proportions. As indicated by the width of LSPR peak in Figure S9, the introduction of EG into DEG tended to make the Ag nanocubes less uniform in size. Taken together, we can conclude that replacement of EG by DEG while keeping other conditions the same is the simplest and most effective approach to the generation of Ag nanocubes with small and uniform sizes.

dx.doi.org/10.1021/ja311503q | *J. Am. Chem. Soc.* 2013, 135, 1941−1951

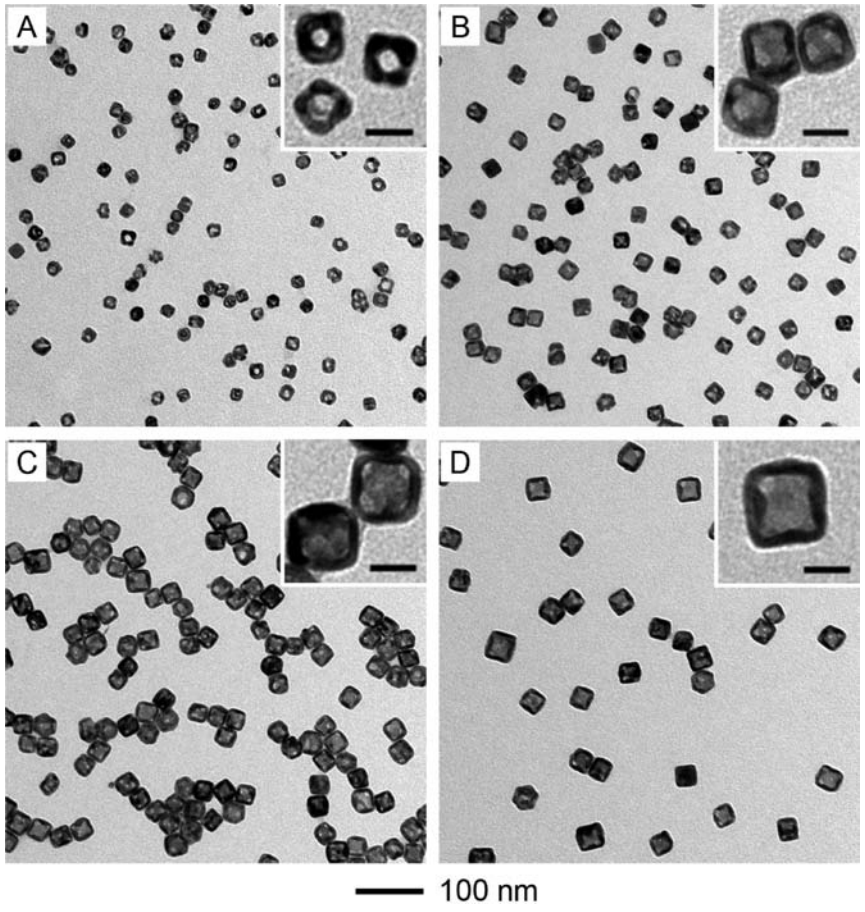

Figure 7. TEM images of typical Au nanocages/frames obtained via a galvanic replacement reaction between $HAuCl_4$ and the small Ag nanocubes with different edge lengths: (A) 18, (B) 23, (C) 28, and (D) 32 nm. The insets are the corresponding high-magnification TEM images, with the scale bars of 20 nm.

Synthesis of Small Au Nanocages/frames with Tunable Optical Properties. From the perspective of applications, single-crystal Ag nanocubes with high purity can serve as seeds for the growth of homogeneous and/or heterogeneous nanocrystals with a variety of shapes, morphologies, and structures, as well as fabrication of bimetallic nanostructures via a galvanic replacement reaction. The resultant nanostructures derived from seeds/templates based on Ag nanocubes are promising candidates for various applications due to their tunable optical, electrical, and catalytic properties.[21−25] For all these applications, it is necessary to achieve high purity, good uniformity, high reproducibility, and robustness for the synthesis of Ag nanocubes, as well as the capability of scaled up production. By using the small Ag nanocubes as templates, Au nanocages/frames with much smaller sizes relative to what has been reported previously could be fabricated via galvanic replacement reaction.[24,48] Moreover, the optical properties of such small Au nanocages/frames could be tailored by simply using Ag nanocubes with different sizes. As shown in Figure 7, hollow cubic nanocages/frames with edge lengths of 21, 26, 31, and 35 nm were obtained corresponding to Ag nanocubes of 18, 23, 28, and 32 nm in edge length, respectively. We also recorded TEM images from the Au nanoframe (21 nm) at different tilted angles relative to the electron beam to confirm its frame-like structure (Figure S10). A detailed discussion on the mechanism of the galvanic replacement reaction can be found in our previous publications.[48]

Figure 8 shows the LSPR extinction spectra of the Au nanocages/frames obtained by pumping specific amounts of

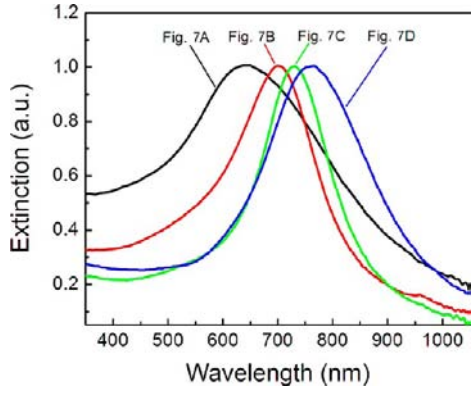

Figure 8. UV−vis spectra taken from aqueous suspensions of the Au nanocages shown in Figure 7 (as marked on the spectra).

$HAuCl_4$ solution into the suspensions of Ag nanocubes with different edge lengths. The LSPR peaks of Au nanocages/frames could be tuned to the maximal wavelengths of 650, 700, 730, and 760 nm when Ag nanocubes with edge lengths of 18, 23, 28, and 32 nm, respectively, were employed as the templates. In principle, the LSPR peak positions of Au

dx.doi.org/10.1021/ja311503q | J. Am. Chem. Soc. 2013, 135, 1941−1951

nanocages/frames can be constantly tuned by adding different amounts of $HAuCl_4$. In other words, their optical properties are highly dependent on the degree of the hollowness in the structure of an Au nanocage/frame. Herein, thanks to an accurate control of the edge length of the Ag templates, we could easily tune the LSPR peak positions of the Au nanocages/frames by using Ag nanocubes with different sizes, meanwhile maintaining a high degree of hollowness in the structures. Such Au nanocages/frames with relatively small sizes, tunable optical properties, and high degrees in hollowness are expected to offer enhanced performance in a range of *in vivo* applications involving drug delivery, optical imaging, and photothermal therapy.

4. CONCLUSION

We have demonstrated a facile and robust method for the synthesis of Ag nanocubes with controlled edge lengths below 30 nm by replacing EG with DEG as both a solvent and a reductant. Compared with EG, DEG possesses a higher viscosity and a lower reducing power owing to the increase in hydrocarbon chain length. As a result, we could achieve a nucleation burst in the early stage to generate a large number of single-crystal Ag seeds and a relatively slow growth rate in the subsequent stage to ensure uniformity and size control. Thus, small Ag nanocubes with uniform, tightly controlled sizes and high purity (typically, >95%) could be reproducibly obtained between batches. With the aid of a UV−vis spectrometer, the edge length of the resultant Ag nanocubes could be readily tuned in the range of 18−32 nm by quenching the reaction at different reaction times. The use of polyol with longer hydrocarbon chains (e.g., TEG or TTEG) only led to the formation of twinned particles with irregular shapes, suggesting that the production of uniform and small Ag nanocubes is highly sensitive to the reaction kinetics. For the first time, we were able to produce uniform sub-20 nm Ag nanocubes on a relatively large scale and in a hydrophilic solution. Using the as-prepared Ag nanocubes as templates, small Au nanocages/frames (21−35 nm) with controllable optical properties were also prepared via a galvanic replacement reaction. The good robustness and reproducibility, as well as the capability for large-scale synthesis, of the present protocol will offer new opportunities of applications for both the Ag nanocubes and Au nanocages. The strategy reported in this article for screening appropriate solvents/reductants in an effort to manipulate the reaction kinetics and thus achieve size control, robustness, and reproducibility, can also be extended to other systems.

■ ASSOCIATED CONTENT

Supporting Information

TEM images of Ag nanocrystals obtained at different temperatures and in the presence of different amounts of PVP; TEM images and UV−vis spectra of Ag nanocrystals obtained in the absence of both NaSH and HCl, or either one of them; photographs showing the setup for the scale-up synthesis and the solution containing Ag nanocubes with an edge length of 23 nm; TEM image of Ag nanocubes prepared using the DEG supplied by a different manufacturer; chemical structures of the polyols, including EG, DEG, TEG, and TTEG; UV−vis spectra taken from the samples shown in Figures 5 and 6; TEM images and the corresponding size distributions of the Ag nanocubes obtained in EG with/without the addition of mPEG; UV−vis spectra and TEM images of the Ag nanoparticles obtained with the addition of formaldehyde as a reductant; UV−vis spectra of Ag nanocubes prepared in mixtures of EG and DEG at different proportions; TEM images of an Au nanoframe at different titled angles. This material is available free of charge via the Internet at http://pubs.acs.org.

■ AUTHOR INFORMATION

Corresponding Author

younan.xia@bme.gatech.edu

Notes

The authors declare no competing financial interest.

■ ACKNOWLEDGMENTS

This work was supported in part by research grants from NIH (R01, CA 138527) and NSF (DMR, 1215034), and startup funds from Georgia Institute of Technology. Y.X. was also partially supported by the World Class University (WCU) program through the National Research Foundation of Korea funded by the Ministry of Education, Science and Technology (R32-20031). As a visiting Ph.D. student from Southwest University, Y.W. was also partially supported by a Fellowship from the China Scholarship Council (CSC). Part of the research was conducted at the Robert P. Apkarian Integrated Electron Microscopy Core of Emory University.

■ REFERENCES

(1) Lewis, L. N. *Chem. Rev.* **1993**, *93*, 2693−2730.
(2) Daniel, M.-C.; Astruc, D. *Chem. Rev.* **2004**, *104*, 293−346.
(3) Anker, J. N.; Hall, W. P.; Lyandres, O.; Shah, N. C.; Zhao, J.; Van Duyne, R. P. *Nat. Mater.* **2008**, *7*, 442−453.
(4) Xia, Y.; Xiong, Y.; Lim, B.; Skrabalak, S. E. *Angew. Chem., Int. Ed.* **2009**, *48*, 60−103.
(5) Talapin, D. V.; Lee, J.-S.; Kovalenko, M. V.; Shevchenko, E. V. *Chem. Rev.* **2010**, *110*, 389−458.
(6) Sönnichsen, C.; Reinhard, B. M.; Liphardt, J.; Alivisatos, A. P. *Nat. Biotechnol.* **2005**, *23*, 741−745.
(7) Rycenga, M.; Cobley, C. M.; Zeng, J.; Li, W.; Moran, C. H.; Zhang, Q.; Qin, D.; Xia, Y. *Chem. Rev.* **2011**, *111*, 3669−3712.
(8) Nie, S.; Emory, S. R. *Science* **1997**, *275*, 1102−1106.
(9) Xia, X.; Zeng, J.; McDearmon, B.; Zheng, Y.; Li, Q.; Xia, Y. *Angew. Chem., Int. Ed.* **2011**, *50*, 12542−12546.
(10) Aslan, K.; Wu, M.; Lakowicz, J. R.; Geddes, C. D. *J. Am. Chem. Soc.* **2007**, *129*, 1524−1525.
(11) Kumar, A.; Vemula, P. K.; Ajayan, P. M.; John, G. *Nat. Mater.* **2008**, *7*, 236−241.
(12) Christopher, P.; Linic, S. *ChemCatChem* **2010**, *2*, 78−83.
(13) Sherry, L. J.; Chang, S.-H.; Schatz, G. C.; Van Duyne, R. P.; Wiley, B. J.; Xia, Y. *Nano Lett.* **2005**, *5*, 2034−2038.
(14) Wiley, B.; Sun, Y.; Mayers, B.; Xia, Y. *Chem.—Eur. J.* **2005**, *11*, 454−463.
(15) Tao, A. R.; Habas, S.; Yang, P. *Small* **2008**, *4*, 310−325.
(16) Wiley, B. J.; Im, S. H.; Li, Z.-Y.; McLellan, J.; Siekkinen, A.; Xia, Y. *J. Phys. Chem. B* **2006**, *110*, 15666−15675.
(17) Tao, A.; Sinsermsuksakul, P.; Yang, P. *Nat. Nanotechnol.* **2007**, *2*, 435−440.
(18) Tao, A.; Sinsermsuksakul, P.; Yang, P. *Angew. Chem., Int. Ed.* **2006**, *45*, 4597−4601.
(19) Rycenga, M.; McLellan, J. M.; Xia, Y. *Adv. Mater.* **2008**, *20*, 2416−2420.
(20) Zeng, J.; Zheng, Y.; Rycenga, M.; Tao, J.; Li, Z.-Y.; Zhang, Q.; Zhu, Y.; Xia, Y. *J. Am. Chem. Soc.* **2010**, *132*, 8552−8553.
(21) Zhang, Q.; Moran, C. H.; Xia, X.; Rycenga, M.; Li, N.; Xia, Y. *Langmuir* **2012**, *28*, 9047−9054.
(22) Xia, X.; Zeng, J.; Oetjen, L. K.; Li, Q.; Xia, Y. *J. Am. Chem. Soc.* **2012**, *134*, 1793−1801.
(23) Xia, Y.; Li, W.; Cobley, C. M.; Chen, J.; Xia, X.; Zhang, Q.; Yang, M.; Cho, E. C.; Brown, P. K. *Acc. Chem. Res.* **2011**, *44*, 914−924.

(24) Chen, J.; McLellan, J. M.; Siekkinen, A.; Xiong, Y.; Li, Z.-Y.; Xia, Y. *J. Am. Chem. Soc.* **2006**, *128*, 14776−14777.
(25) Chen, J.; Wiley, B.; McLellan, J.; Xiong, Y.; Li, Z.-Y.; Xia, Y. *Nano Lett.* **2005**, *5*, 2058−2062.
(26) Sun, Y.; Xia, Y. *Science* **2002**, *298*, 2176−2179.
(27) Im, S. H.; Lee, Y. T.; Wiley, B.; Xia, Y. *Angew. Chem., Int. Ed.* **2005**, *44*, 2154−2157.
(28) Lee, Y. T.; Im, S. H.; Wiley, B.; Xia, Y. *Chem. Phys. Lett.* **2005**, *411*, 479−483.
(29) Siekkinen, A. R.; McLellan, J. M.; Chen, J.; Xia, Y. *Chem. Phys. Lett.* **2006**, *432*, 491−496.
(30) Skrabalak, S. E.; Au, L.; Li, X.; Xia, Y. *Nat. Protoc.* **2007**, *2*, 2182−2190.
(31) Skrabalak, S. E.; Wiley, B. J.; Kim, M.; Formo, E. V.; Xia, Y. *Nano Lett.* **2008**, *8*, 2077−2081.
(32) Zhang, Q.; Cobley, C.; Au, L.; McKiernan, M.; Schwartz, A.; Wen, L.-P.; Chen, J.; Xia, Y. *ACS Appl. Mater. Interfaces* **2009**, *1*, 2044−2048.
(33) Zhang, Q.; Li, W.; Wen, L.-P.; Chen, J.; Xia, Y. *Chem.—Eur. J.* **2010**, *16*, 10234−10239.
(34) Zhang, Q.; Li, W.; Moran, C.; Zeng, J.; Chen, J.; Wen, L.-P.; Xia, Y. *J. Am. Chem. Soc.* **2010**, *132*, 11372−11378.
(35) Yu, D.; Yam, V. W.-W. *J. Am. Chem. Soc.* **2004**, *126*, 13200−13201.
(36) Chen, H.; Wang, Y.; Dong, S. *Inorg. Chem.* **2007**, *46*, 10587−10593.
(37) Zhang, Q.; Huang, C. Z.; Ling, J.; Li, Y. F. *J. Phys. Chem. B* **2008**, *112*, 16990−16994.
(38) Ma, Y.; Li, W.; Zeng, J.; McKiernan, M.; Xie, Z.; Xia, Y. *J. Mater. Chem.* **2010**, *20*, 3586−3589.
(39) Gittins, D. I.; Caruso, F. *Angew. Chem., Int. Ed.* **2001**, *40*, 3001−3004.
(40) Wang, Y.; Wong, J. F.; Teng, X.; Lin, X. Z.; Yang, H. *Nano Lett.* **2003**, *3*, 1555−1559.
(41) Wei, G.-T.; Yang, Z.; Lee, C.-Y.; Yang, H.-Y.; Wang, C. R. C. *J. Am. Chem. Soc.* **2004**, *126*, 5036−5037.
(42) Kim, D. Y.; Li, W.; Ma, Y.; Yu, T.; Li, Z.-Y.; Park, O. O.; Xia, Y. *Chem.—Eur. J.* **2011**, *17*, 4759−4764.
(43) Lee, C.-L.; Wan, C.-C.; Wang, Y.-Y. *Adv. Funct. Mater.* **2001**, *11*, 344−347.
(44) Zheng, Y.; Tao, J.; Liu, H.; Zeng, J.; Yu, T.; Ma, Y.; Moran, C.; Wu, L.; Zhu, Y.; Liu, J.; Xia, Y. *Small* **2011**, *7*, 2307−2312.
(45) Zhang, Q.; Xie, J.; Yu, Y.; Yang, J.; Lee, J. Y. *Small* **2010**, *6*, 523−527.
(46) Sun, T.; Teja, A. S. *J. Chem. Eng. Data* **2003**, *48*, 198−202.
(47) Sagdeev, D. I.; Fomina, M. G.; Mukhamedzyanov, G. K.; Abdulagatov, I. M. *J. Chem. Thermodyn.* **2011**, *43*, 1824−1843.
(48) Sun, Y.; Xia, Y. *J. Am. Chem. Soc.* **2004**, *126*, 3892−3901.